

EXPLORING THE LIMITS OF TERRESTRIAL LASER SCANNERS ON AEROSPACE MATERIALS

Kate Pexman and Stuart Robson

Department of Civil, Environmental and Geomatic Engineering, University College London
katherine.pexman.21@ucl.ac.uk

KEY WORDS: Terrestrial Laser Scanning, Point Clouds, Registration, Feature Extraction, Aerospace Manufacturing

ABSTRACT:

Terrestrial laser scanners are powerful measurement devices commonly used for 3D modelling tasks generating large volumes of data with fast acquisition as a first priority. However, these scanners can alternatively be used to produce near real-time, engineering quality spatial data concerning the changing state of manufactured components. This paper provides a comprehensive analysis of two terrestrial laser scanners capturing aerospace materials and components, and their associated quality measures. In order to explore the limitations of the tested TLS instruments, a mechanical jig was designed incorporating both a rotation and translation stage. This study involved three elements of a point cloud processing workflow: data capture, registration and feature extraction. Sphere-based 7DoF registration is applied using two different commercially available software packages with varying levels of user control. To analyse the quality of the registration, control points extracted from captured point clouds were compared to nominal values measured using a laser tracker. The quality of the registration was consistent, with differences kept between 0.4 mm and 0.6 mm. To evaluate the quality of the captured point clouds, two different tests were conducted. This included planar fit tests on an aluminium drilling template, and sphere fitting tests on white 1.5" spherical targets in magnetic nests. One half of the aluminium drilling template was coated with matte spray to reduce erroneous laser reflections. Finally, the registered point clouds were input to a developed algorithm which automatically extracted drilling holes from the drilling template. Previous scanning work performed on aerospace materials showed evidence of optical rattling caused by high intensity reflections from the interior holes in a drilling template. Further exploration showed that the amount of optical rattle varies systematically with incidence angle. This work demonstrates a systematic offset in the location of extracted hole centres in the drilling template. This offset is dependent on laser incidence angle, and can therefore be accounted for when locating manufacturing components from a known scanning position.

1. INTRODUCTION

Terrestrial laser scanners (TLS) are high fidelity measurement devices that work quickly and can capture a huge amount of spatial information. These measurement devices are commonly used for tasks such as building modelling [1], reverse engineering [2], and change monitoring [3], among others. In contrast, the vast majority of measurements made during a high-precision measurement task such as aerospace manufacturing requires sub-millimetre level control [4], [5]. This is typically achieved using laser trackers or various types of Coordinate Measuring Machines (CMM). With a CMM, components can be placed inside the machine's measurement space and coordinated with a high degree of precision either by touch probe or scanning head. However, an obvious downside in using CMMs is the lack of ability to deal with large objects, an important factor in aerospace manufacturing.

For aerospace manufacturing tasks, measurements are often made manually using various types of hand held gauges. These types of measuring strategies can produce measurements with sub-millimetre level precision. However, it is difficult to capture a large number of measurements efficiently and reliably with a manual strategy. Aerospace component dimensions exacerbate the inefficiency of relying on CMM or manual measurements. This provides the catalyst of this work: the exploration of TLS capabilities for high-precision, large-volume manufacturing measurements. The work presented herein focuses on the comparison of two terrestrial laser scanners in manufacturing environments, as well as the influence of incidence angle when scanning materials with high reflectivity.

Performing the same tasks with multiple scanners, under the same environmental conditions and set up, allows for meaningful and insightful comparisons. One of the first explorations of laser scanner accuracy came from [6], where TLS from different manufacturers were compared by scanning planar surfaces with varying reflectivity and range. A more recent example where multiple terrestrial laser scanners were examined can be found in [7], where various tests were performed to explore the distance accuracy of five similar TLS. A review of the work done in the last two decades to compare terrestrial laser scanners was presented in [8], where the ongoing work of many research labs was evaluated.

The varied optical surface characteristics of aerospace components means they can be difficult to scan, commonly producing erroneous returns. This is exacerbated in a real-world scanning scenario where components are scanned from different incidence angles over a large volume. At large incidence angles, phenomena such as optical rattle can occur on confined, highly reflective surfaces, causing an over-estimation of path length. Optical rattle occurs when a laser pulse internally reflects inside an object before emerging and reflecting back to the scanner. In our experiments, the laser pulse rattles around inside the cylindrical holes in the drilling template until it eventually exits and returns to the scanner. The resulting increase in path length is a function of the laser beam angle and object geometry altering cylindrical drilling holes into lobed objects in the output point cloud such as that seen in Figure 1. An in-depth analysis on the effect of incidence angle and distance on terrestrial laser scanner measurements was produced by [9], specifically related

to intensity measurements. The majority of work that explores the effect of changing incidence angle focuses on correcting the intensity values in the point cloud [10]–[13] rather than the range. Identifying and characterizing these erroneous returns allows for a higher degree of accuracy in feature extraction.

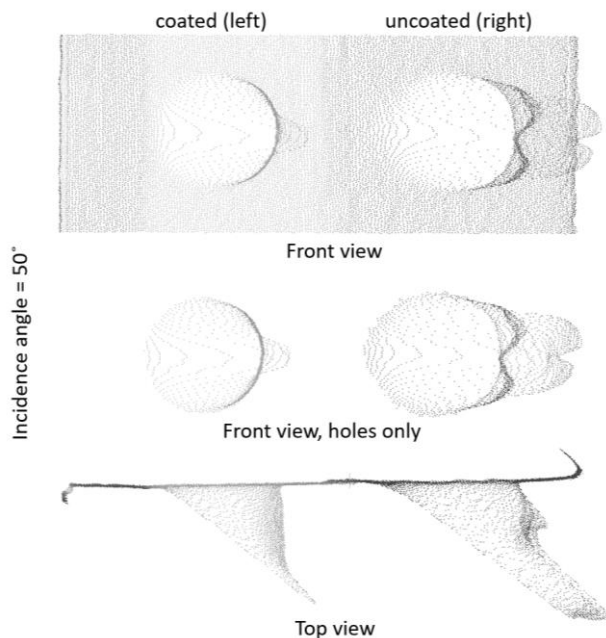


Figure 1. Example of optical rattling in a cylindrical hole

Plenty of literature in the study of high-precision measurement is available, however papers typically cover laser line scanners and CMMs. The study presented herein focuses specifically on the use of terrestrial laser scanners for high-precision, large-volume measurement, and therefore will not include a complete review of any additional scanners or measurement devices.

Once a complex scene has been captured by a terrestrial laser scanner, the output point clouds from different scanner locations must be registered together. This is because an entire 3D representation of an object or component can rarely be captured from a single viewpoint due to line of sight occlusions. There has been significant work on both targeted and targetless registration of point clouds, all of which cannot be covered here. This work focusses on the sphere-based registration of point clouds, as previously exemplified by [14]–[16], among others. The tests undertaken used purpose-made 1.5” spheres for registration, interchangeable with sphere mounted retroreflector (SMR) targets used by laser trackers.

When point clouds have been registered together, useful information can be extracted from them. In service of moving towards automated manufacturing, this information could include component locations and orientations. If a near real-time version of the aerospace manufacturing environment can be captured, progress and quality monitoring can be performed by locating specific manufacturing components and tools. The example explored in this work locates drilling templates on the surface of an airplane wing section. This is done by automatically finding the circular outlines of the holes in the drilling template. Previous work on circle extraction from point clouds includes circle fitting [17] and ellipse identification [18], mainly used for circular target extraction and cylindrical pipe fitting. In an aerospace specific application, point clouds have

been used to find aircraft fasteners [19], and tiny engine nacelle holes [20].

This work explores data capture, registration and feature extraction. Quality measures have been produced for all three elements of a laser scanning workflow, which will subsequently be discussed. The paper is outlined as follows: Section 2 explains the methodology used to explore the successes and shortcomings of both scanners on different aerospace-specific scanning tests; Section 3 describes the results obtained from these tests; and finally, Section 4 concludes the research with discussion of next steps.

2. METHOD

This research was designed to explore the limits of TLS and discover levels of achievable precision and accuracy in an aerospace manufacturing application. Two terrestrial laser scanners were chosen. Both are mainstream, phase-based scanners capable of producing high quality point clouds. The tests were designed to examine both the scanning performance and registration performance of the two instruments. One key difference was that Scanner A was limited in terms of user control when it came to processing the captured scans. The processing mostly functioned as a ‘black box’ with embedded filters that could not be changed by the user. In contrast, significantly more user control was available for Scanner B. For Scanner B, all filtering (distance, intensity, etc) was removed in order to access the most raw version of the captured point cloud. Additionally, two different software were used to perform sphere extraction and perform registration. The two software will be referred to as SA and SU. Both scanners could use SA to extract spheres, which used the ASTM E3125-17 [21] to fit a sphere to each set of extracted points. However, the SU software is proprietary and could therefore only be used on Scanner B.

In order to have a baseline with which to compare the two laser scanners, a Leica AT960MR Laser Tracker was used to provide reference values. The laser tracker can make point measurements as well as surface contact measurements with a SMR or tracked touch probe, both of which will be used to compare the laser scanners. The laser tracker has uncertainty in the tens of microns, making it an order of magnitude more precise than either of the laser scanners. Although the laser tracker cannot be considered to produce ‘true’ values, it gives an indication as to laser scanner performance in each of the evaluation tests.

2.1 Scanning

Both scanners captured the mechanical drilling jig as well as a complete 5m section of an aircraft wing. Each scanner was positioned at approximately the same location and at a height of 1.2 metres. Scanner A was placed upon a light-weight camera tripod, while Scanner B was placed upon a heavy-duty tripod. Figure 2 shows the drilling template on the mechanical jig along with some of the spherical targets in magnetic nests.

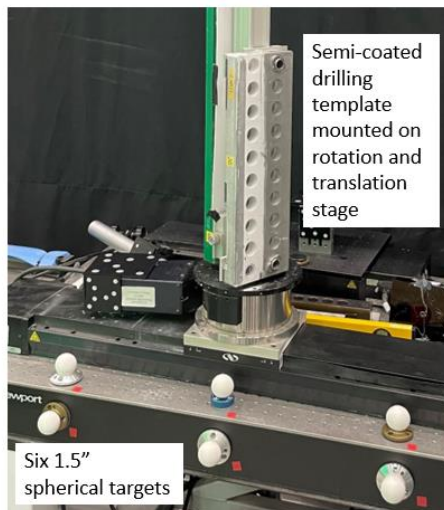


Figure 2. Mechanical jig with semi-coated drilling template and six spherical targets in different magnetic nests

As mentioned, a mechanical jig including a rotation stage sitting atop a translation stage was designed in order to vary the incidence angle of the drilling template in a precise and repeatable manner. The jig was affixed to the top of a metrology table. Both the translation stage and the rotation stage can be controlled, however, for this work only the rotation stage was altered. The rotation stage was placed on the translation stage and a vertically mounted beam with multiple drilling templates was affixed to the rotation stage. A vertical orientation was used in order to mimic the orientation of drilling templates in a real aerospace manufacturing environment. At each 10 degree increment of the rotation stage, both TLS were used to capture the drilling template. This process was repeated with the drilling template in each orientation on the rotation stage.

One side of the drilling template was coated with a matte spray to reduce high intensity reflections from the metallic surface. These reflections cause gaps in the captured point clouds at low incidence angles and contribute significantly to optical rattle. Changing the optical surface material properties in such a way as to improve the scanning results is a common but undesirable strategy in design-for-measurement, where component properties are optimized to improve their measurability.

To scan the mechanical drilling jig, the scanner was placed at a distance of 2 metres from the template. This distance was chosen as per the work done in [22], to optimize sphere extraction and minimize registration errors. Once the scanner was in position, the drilling template was scanned at an incidence angle of 0 degrees. The drilling jig was then rotated to an incidence angle of 70 degrees and scanned. The drilling jig was then rotated by 10 degree increments and scanned until the drilling jig reached -70 degrees. Finally, the drilling jig was scanned again at an incidence angle of 0 degrees to close the loop. The same process was followed for both tested scanners. This produced a total of 17 scans per scanner.

Additionally, scans were captured of an Airbus A321 wing section in the UCL lab at HereEast, as shown in Figure 3. The wing was scanned by both scanners from all four corners. Spherical targets were placed around the area, located in metrology nests both on the wing section and on the concrete floor. These provided a physical coordinate system to be used in the registration process.



Figure 3. Wing section with multiple drilling templates, spherical targets and scale bar visible

2.2 Sphere-based Registration

Once the scans were captured, a sphere-based registration strategy was used. This involved the automatic extraction of the 1.5" white matte spheres from each individual point cloud. For Scanner A this was done in SA, and for Scanner B this was done using the scanner's proprietary software, SU, as well as SA.

Once the centre points of each sphere were extracted they could be matched back to a network of control points measured using the Leica AT960MR Laser Tracker. In this work, the control points measured by the laser tracker are considered as the reference value. Using the network of known control points, a 7 degrees of freedom (DoF) best fit transformation was applied to each individual scan. For the complete wing scans, the location and distribution of the targets varied within the scanning volume. The location of the targets remained consistent for the drilling jig scans as the scanner did not move.

Once registration had been performed, the centre of the spheres in each registered scan could be compared to the reference network of control points measured by the laser tracker. This gave an indication of the precision of each scan, as well as the repeatability of the scan at each incremental rotation of the drilling jig. These results will be discussed in Section 3.

2.3 Planar Fit

One side of the drilling template mounted on the drilling jig was coated with a matte spray. This reduced the level of high-intensity reflection from the metallic surface of the drilling template. Both the surface of the template as well as the interior of the drilling holes were coated.

In order to further compare Scanner A and Scanner B when scanning a metallic surface at varying incidence angles, the quality of the planar fit on the surface of the drilling template

was evaluated. The top surface of the drilling template was assumed to be planar.

At each 10 degree rotation increment, a section of the planar top surface was extracted on both the coated and the uncoated sides of the drilling template. A planar feature was fit to the two groups of selected points and the root mean square (RMS) value was computed as an accuracy indicator of the reconstructed planar section. This helped to illustrate the quality of the planar section captured by each scanner at each incremental rotation of the mechanical drilling jig. These results will be discussed in Section 3.

2.4 Sphere Fit

Similar to the planar fit test, a sphere fit test was performed to evaluate the presence of noise and outliers on the surface of the target spheres. In each of the 17 scans captured of the mechanical drilling jig, the six spherical targets in nests were extracted and analysed. The group of points in the point cloud that made up each target sphere were fitted to a spherical model and their RMS and maximum deviation were reported. These results are discussed in Section 3.

As seen in Figure 2, three of the spherical targets are sitting in nests on the front of the metrology table, and three of the nests are sitting on top of the metrology table. When the scanner was approximately 2 metres from the mechanical jig, the spherical targets appeared in the point cloud in aerial view (front of table) and profile view (on top of table). Importantly, when the spheres are in profile view, approximately 15% of the sphere is obscured by the metrology nest. In addition, the type, colour and size of metrology nests were varied between the targets. This test was performed to investigate whether either of the automatic sphere extraction techniques had any bias based on either sphere view or nest type. These results will be discussed in Section 3.

2.5 Drilling template hole extraction

Once the point clouds had been captured, registered, and analysed, meaningful information could be extracted. This involved designing an algorithm that could automatically locate the centre of each hole on the drilling template. The ability to precisely locate the drilling template during manufacture can allow for near real-time progress monitoring and drilling template placement correction. The algorithm was originally designed in [22], however in this work it has been improved to account for larger variations incidence angle.

At each incremental rotation of the mechanical drilling jig, the scanned drill hole centres were located and compared to the drill hole centres measured using the laser tracker. Drill hole centres were extracted on both the coated and uncoated sides of the drilling template, in order to evaluate the effectiveness of the matte coating in reducing outliers and improving hole centre estimation. The results are discussed in Section 3.

3. RESULTS

3.1 Registration results

Registration was performed using a 7DoF adjustment between directly measured laser tracker sphere centres and estimated laser scanned sphere centres. One assessment of the quality of the sphere-based registration is shown in Figure 4. Both Scanner A and Scanner B are represented, as well as the two

different sphere extraction software, SA and SU. The Scanner A results could not use the SU software because it was proprietary and only compatible with Scanner B.

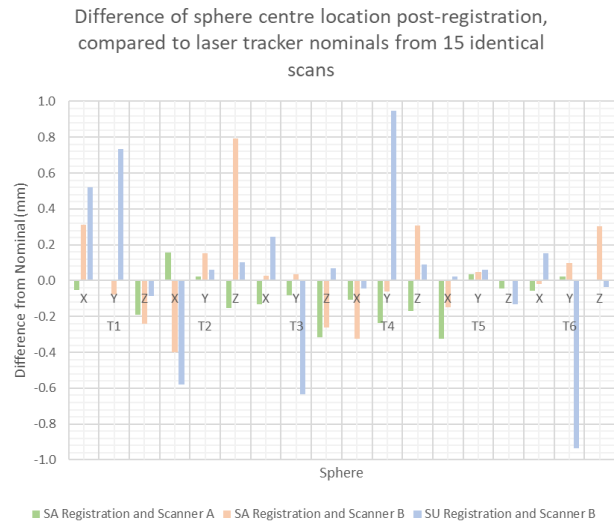


Figure 4. Quality evaluation of sphere-based registration

The results presented in Figure 4 show the difference between the centre of the scanned target spheres and the centre of the target spheres measured by the laser tracker. The differences are broken down into X, Y, and Z components for all six spherical targets on the mechanical jig. The most consistent results came from Scanner A using the SA registration software, which can be seen by the small relative differences between laser scanned sphere centres and laser tracked sphere centres. This indicates that Scanner A using SA software produces accurate estimations of sphere centres. Significant spikes are seen for Scanner B in both registration software. The spikes for Scanner B with SU registration are largest in the Y direction, however for Scanner B with SA the spikes are in the X and Z directions.

In addition to assessing the quality of each scan, repeatability could be evaluated by examining the standard deviation of each sphere location in each scan. Aside from the incremental rotation of the drilling jig, all other elements of the scanning setup (scanner location, target location, environmental aspects) were kept consistent. The repeatability is evaluated in 3D in Figure 5.

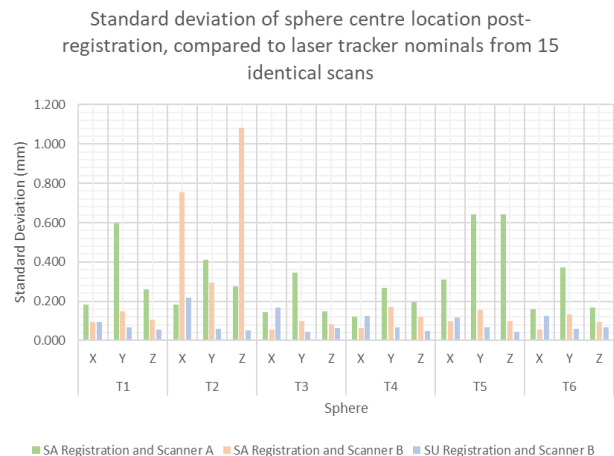


Figure 5. Repeatability of sphere-based registration

The results presented in Figure 5 show that the repeatability of Scanner A is worse than Scanner B, in both sphere extraction software. Scanner A had a higher standard deviation of sphere centre location, indicating lower repeatability confidence from one scan to another. The two registration tests indicate that although Scanner A is more accurate than Scanner B, Scanner B is more precise than Scanner A.

3.2 Planar fit results

The purpose of testing the planar fit was to examine the quality of the planar sections with varying incidence angle for both Scanner A and Scanner B. Planar sections on both the coated and uncoated sides of the template were evaluated in all rotations from both scanners. Figure 6 shows the RMS values of the points fitted to a planar model from both scanners on both the coated and uncoated sides of the drilling template. The graph illustrates how the drilling template changes as it is rotated around the mechanical jig and the incidence angle changes between the planar surface and the scanner.

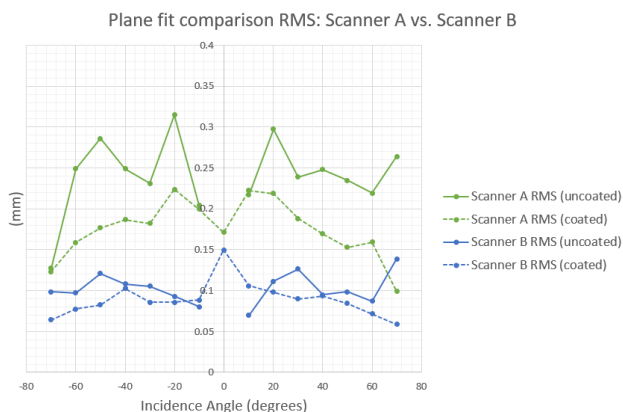


Figure 6. Planar fit tests for Scanner A & Scanner B

Scanner B had a clear advantage when compared to Scanner A in the planar fit tests. RMS values were observed between 0.05 mm and 0.35 mm for planar fit. An improvement is evident for the planar sections fit to the spray coated side of the drilling template, for almost all incidence angles. Notably, the presence of matte coating improves the quality of the planar surface for Scanner A more than for Scanner B. There is no value at the zero incidence angle for either Scanner A or Scanner B on the uncoated side of the template because the reflection produced intensity values so high that they caused gaps in the captured point cloud, meaning no planar section could be fit.

3.3 Sphere fit results

Two tests were conducted to analyse the quality of the sphere fit. The first was to examine whether the orientation (aerial vs profile) or type and size of nest (blue, silver, gold) had an effect on the sphere fit from the point clouds produced by either Scanner A or Scanner B. Mathematically, a sphere should appear the same from all angles, however it was important to ensure that the orientation of the spherical targets or the nest type was not causing a bias in the quality of the sphere fitting. Varying the orientation of the spherical targets had negligible effect on the quality of their extraction. In addition, varying the physical form and colour of the metrology nest did not have a consistent effect on the sphere fitting for the point clouds produced by either Scanner A or Scanner B.

In the second test, sphere fitting was compared between the two scanners. This was done by analysing the RMS value of the points on each captured sphere in the point cloud. The RMS value was produced by fitting the sphere points in the point cloud to a mathematical sphere. The maximum deviation of the points from the spherical model is also shown in Figure 7.

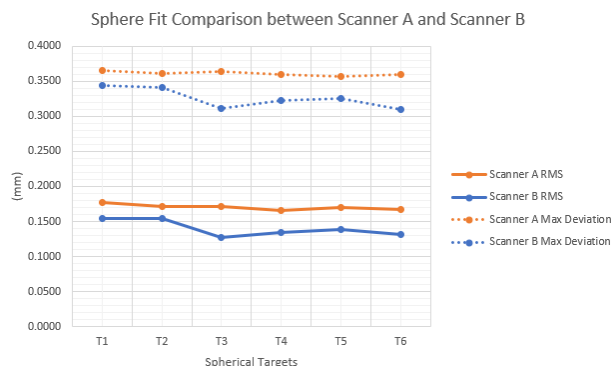


Figure 7. Sphere fit tests for Scanner A & Scanner B

RMS values were observed between 0.1 mm and 0.2 mm for sphere fit and maximum deviation from the sphere model were between 0.3 mm and 0.4 mm. Scanner B had an advantage when compared to Scanner A in the sphere fit tests, with a smaller RMS value for all six spherical targets. However, this advantage in RMS from Scanner B to Scanner A is only 0.03 mm, which is not a significant improvement.

3.4 Drilling template hole extraction results

In order to evaluate the influence of incidence angle when scanning an aerospace component such as a metallic drilling template, the drilling holes were extracted from the template and compared to reference values. The reference values of the hole centres in the drilling template were measured using the laser tracker and a SMR target at each 10° orientation increment. The diameters of the holes were checked using callipers and assumed to be cylindrical.

The main interest in testing the incidence angle of the drilling template came from the presence of erroneous points inside the drill holes. Optical rattle occurred inside the drill holes, meaning as the laser pulse entered the hole and came into contact with the curved, highly reflective surface, it did not reflect directly back to the scanner. Instead, it 'rattled' around inside of the cylindrical hole before eventually exiting the cylinder and returning to the scanner. This caused an increase in path length and an inaccurate representation of the inside of the cylindrical drill hole. These inaccuracies in the point cloud could lead to biases in the estimation of the hole centres in the automatic drill hole extraction algorithm. An example of the variation of optical rattle with incidence angle is shown in the schematic in Figure 8.

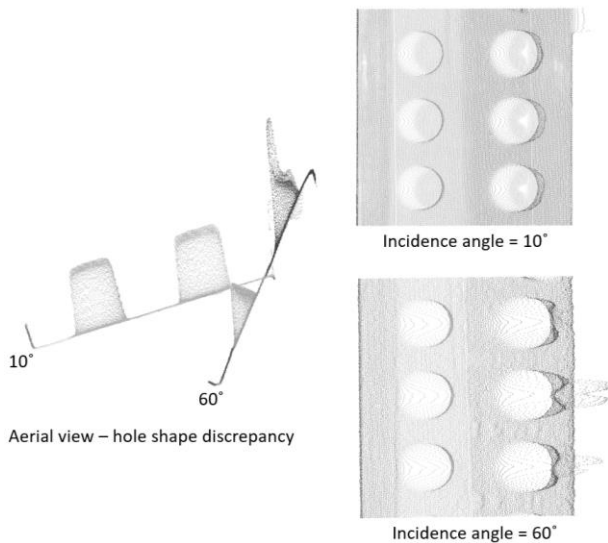


Figure 8. Variation of incidence angle when scanning drilling template; optical rattle effect

The reader is asked to refer to [22] where the extraction algorithm has been described in detail. An example result of the hole extraction algorithm is shown in Figure 9.

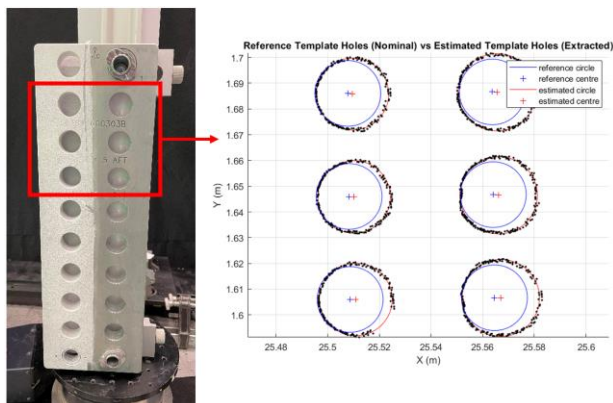


Figure 9. Drilling template hole extraction result in working coordinate frame

The algorithm was run to extract the hole centres from the point cloud at each 10 degree increment. The results of the hole centre extraction are shown in Figure 10.

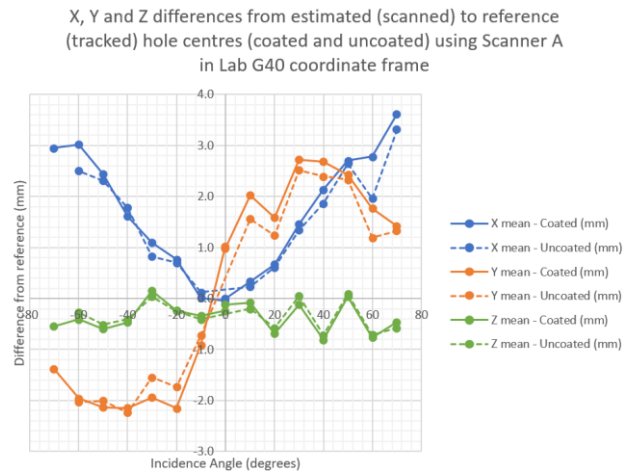


Figure 10. Systematic offset of drilling template hole extraction through varying incidence angles in real-world (Lab G40) coordinate frame

The differences shown are between the centres of the extracted holes and those measured by the laser tracker, in the axes of the G40 lab coordinate frame. In this coordinate frame, Z is vertical, X is approximately along the axis of the translation frame, and Y is approximately towards the drilling jig from the laser scanner. This was done for both scanners, each of which obtained similar systematic results.

It is evident from Figure 10 that there is a systematic effect in the differences as the drilling template rotates through the incidence angles. In all three directions, the difference from the reference becomes small when the incidence angle tends to zero. However, at a zero incidence angle, the uncoated side of the template was not represented in the point cloud due to gaps caused by high intensity returns. The differences in the X direction and the Y direction follow relatively predictable curves. In the Y direction, the difference of the hole centres from the nominal begins to decrease around 60 degrees, while in the X direction it appears as though the error continues to increase. The rotation of the drilling template does not have an impact on the centre of the holes in the Z direction, as it is consistently measured just between 0 and 1 mm. Perhaps most interestingly, the coated and the uncoated hole centres follow very similar trends. In all three directions there is no obvious improvement in the hole centre estimation when the drilling template is coated with the matte spray.

4. CONCLUSIONS AND FUTURE WORK

The work conducted herein explores some of the limits of terrestrial laser scanners when recording metallic aerospace surfaces. Point clouds from terrestrial laser scanners are registered to a network of known points measured by a laser tracker using a 7DoF best fit transformation. Two mainstream, phase-based scanners are tested in a variety of ways, including spherical and planar model fitting. Overall, registration errors are below 1 mm, and fitting errors are all kept around or under 0.4 mm. This indicates a wide potential of using terrestrial laser scanning for high precision imaging tasks such as aerospace manufacturing. A mechanical jig is designed to vary the incidence angle of a common aerospace component, a drilling template, in order to explore the presence of optical rattle. Through various tests it is shown that the amount of optical rattle occurring within a metallic cylinder varies systematically with incidence angle.

Across the majority of tests, Scanner B outperformed Scanner A. However, for sphere-based registration the results of Scanner B were more precise but less accurate than Scanner A. The increased user control of Scanner B software was beneficial for reducing the amount of filtering that was automatically applied. In this way, it was possible to access a more ‘raw’ version of the captured point cloud. The main advantage of adding a matte coating to the surface of the drilling template is the ability to scan at a zero incidence angle. However, hole centre measurement based on the developed algorithm experiences an insignificantly small advantage from the presence of matte coating at all incidence angles other than zero.

Future work will involve the modelling of the erroneous points inside the drilling template holes. This could be done by quantifying the relationship between incidence angle and hole offset, and correcting back to a known model of a cylindrical hole.

ACKNOWLEDGEMENTS

This work was conducted with the support of UCL EPSRC scholarship, as well as support from Airbus.

REFERENCES

- [1] K. Pexman, D. D. Lichti, and P. Dawson, “Automated Storey Separation and Door and Window Extraction for Building Models from Complete Laser Scans,” *Remote Sens.*, vol. 13, no. 17, p. 3384, Aug. 2021, doi: 10.3390/rs13173384.
- [2] Y. Yang, H. Fang, Y. Fang, and S. Shi, “Three-dimensional point cloud data subtle feature extraction algorithm for laser scanning measurement of large-scale irregular surface in reverse engineering,” *Measurement*, vol. 151, p. 107220, Feb. 2020, doi: 10.1016/j.measurement.2019.107220.
- [3] P. Dawson, J. Brink, A. Farrokhi, F. Jia, and D. Lichti, “A method for detecting and monitoring changes to the Okotoks Erratic – ‘Big Rock’ provincial historic site,” *J. Cult. Herit. Manag. Sustain. Dev.*, vol. ahead-of-print, no. ahead-of-print, Jan. 2022, doi: 10.1108/JCHMSD-10-2021-0183.
- [4] P. Vichare, O. Martin, and J. Jamshidi, “Dimensional management for aerospace assemblies: framework implementation with case-based scenarios for simulation and measurement of in-process assembly variations,” *Int. J. Adv. Manuf. Technol.*, vol. 70, no. 1–4, pp. 215–225, Jan. 2014, doi: 10.1007/s00170-013-5262-9.
- [5] R. Rubio, L. Granero, M. Sanz, J. García, and V. Micó, “Analysis and 3D inspection system of drill holes in aeronautical surfaces,” presented at the SPIE Optical Metrology, P. Lehmann, W. Osten, and A. Albertazzi Gonçalves, Eds., Munich, Germany, Jun. 2017, p. 1032948. doi: 10.1117/12.2270302.
- [6] W. Boehler and A. Marbs, “Investigating Laser Scanner Accuracy,” 2003.
- [7] T. P. Kersten and M. Lindstaedt, “Geometric accuracy investigations of terrestrial laser scanner systems in the laboratory and in the field,” *Appl. Geomat.*, vol. 14, no. 2, pp. 421–434, Jun. 2022, doi: 10.1007/s12518-022-00442-2.
- [8] B. Muralikrishnan, “Performance evaluation of terrestrial laser scanners—a review,” *Meas. Sci. Technol.*, vol. 32, no. 7, p. 072001, Jul. 2021, doi: 10.1088/1361-6501/abdae3.
- [9] S. Kaasalainen, A. Jaakkola, M. Kaasalainen, A. Krooks, and A. Kukko, “Analysis of Incidence Angle and Distance Effects on Terrestrial Laser Scanner Intensity: Search for Correction Methods,” *Remote Sens.*, vol. 3, no. 10, Art. no. 10, Oct. 2011, doi: 10.3390/rs3102207.
- [10] A. Kukko, S. Kaasalainen, and P. Litkey, “Effect of incidence angle on laser scanner intensity and surface data,” *Appl. Opt.*, vol. 47, no. 7, p. 986, Mar. 2008, doi: 10.1364/AO.47.000986.
- [11] A. Krooks, S. Kaasalainen, T. Hakala, and O. Nevalainen, “Correction of Intensity Incidence Angle Effect in Terrestrial Laser Scanning,” *ISPRS Ann. Photogramm. Remote Sens. Spat. Inf. Sci.*, vol. II-5/W2, pp. 145–150, Oct. 2013, doi: 10.5194/isprsannals-II-5-W2-145-2013.
- [12] K. Tan and X. Cheng, “Intensity data correction based on incidence angle and distance for terrestrial laser scanner,” *J. Appl. Remote Sens.*, vol. 9, no. 1, p. 094094, Sep. 2015, doi: 10.1117/1.JRS.9.094094.
- [13] D. Bolkas, “Terrestrial laser scanner intensity correction for the incidence angle effect on surfaces with different colours and sheens,” *Int. J. Remote Sens.*, vol. 40, no. 18, pp. 7169–7189, Sep. 2019, doi: 10.1080/01431161.2019.1601283.
- [14] P. Rachakonda *et al.*, “Methods and considerations to determine sphere center from terrestrial laser scanner point cloud data,” *Meas. Sci. Technol.*, vol. 28, no. 10, p. 105001, Oct. 2017, doi: 10.1088/1361-6501/aa8011.
- [15] M. Zhang, “Accurate Sphere Marker-Based Registration System of 3D Point Cloud Data in Applications of Shipbuilding Blocks,” *J. Ind. Intell. Inf.*, vol. 3, no. 4, 2015, doi: 10.12720/jiii.3.4.318-323.
- [16] Y. Wang, H. Shi, Y. Zhang, and D. Zhang, “Automatic registration of laser point cloud using precisely located sphere targets,” *J. Appl. Remote Sens.*, vol. 8, no. 1, p. 083588, Jul. 2014, doi: 10.1117/1.JRS.8.083588.
- [17] A. Nurunnabi, Y. Sadahiro, and D. F. Laefer, “Robust statistical approaches for circle fitting in laser scanning three-dimensional point cloud data,” *Pattern Recognit.*, vol. 81, pp. 417–431, Sep. 2018, doi: 10.1016/j.patcog.2018.04.010.
- [18] R. Maalek and D. D. Lichti, “Robust detection of non-overlapping ellipses from points with applications to circular target extraction in images and cylinder detection in point clouds,” *ISPRS J. Photogramm. Remote Sens.*, vol. 176, pp. 83–108, Jun. 2021, doi: 10.1016/j.isprsjprs.2021.04.010.
- [19] Q. Xie *et al.*, “Aircraft Skin Rivet Detection Based on 3D Point Cloud via Multiple Structures Fitting,” *Comput.-Aided Des.*, vol. 120, p. 102805, Mar. 2020, doi: 10.1016/j.cad.2019.102805.
- [20] H. Tang, L. Zhou, Y. Liu, and J. Wang, “Tiny hole inspection of aircraft engine nacelle in 3D point cloud via robust statistical fitting,” *Measurement*, vol. 196, p. 111250, Jun. 2022, doi: 10.1016/j.measurement.2022.111250.
- [21] E57 Committee, “Standard Test Method for Evaluating the Point-to-Point Distance Measurement Performance of Spherical Coordinate 3D Imaging Systems in the Medium Range,” ASTM International, 2017. doi: 10.1520/E3125-17.
- [22] K. Pexman and S. Robson, “Registration And Feature Extraction From Terrestrial Laser Scanner Point Clouds For Aerospace Manufacturing,” *Int. Arch. Photogramm. Remote Sens. Spat. Inf. Sci.*, vol. XLVIII-2/W2-2022, pp. 119–126, Dec. 2022, doi: 10.5194/isprs-archives-XLVIII-2-W2-2022-119-2022.